

CHAPTER 4.

DESIGN of EXPERIMENTAL INDUCTION MOTOR DRIVE SYSTEM.

4.1 - Introduction.

In previous chapters it has been introduced the theoretical study of both the DTC and the FLDTTC. Also, these studies have been verified by means of simulations. Next chapter deals with the implementation of both versions of Direct Torque Control. Previously, a drive system has been firstly design and then used.

This chapter is focused on the architecture of the full drive system and the motor workbench, being entirely described in detail its main features. Also, the present chapter deals with the program tools and the organisation of the different tasks. (All programs are listed in section A2).

Design of experimental induction motor drive system.

A brief description of the real implemented programs and its main routines are explained. Finally, some DTC and FLDTTC real simulations, which have been realised taking into account the real drive with all its delays and the finally used sampling period ($166\mu\text{s}$), are shown.

4.2 - Induction motor drive architecture.

Figure 4.1 shows the workbench, which has been fully set up for the present thesis. All the system drive has been specially developed not only for this thesis but also for any implementation of further research in the topic of motor drives. Therefore, this workstation is supposed to be very versatile as well as powerful [BED 2] [BED 3].

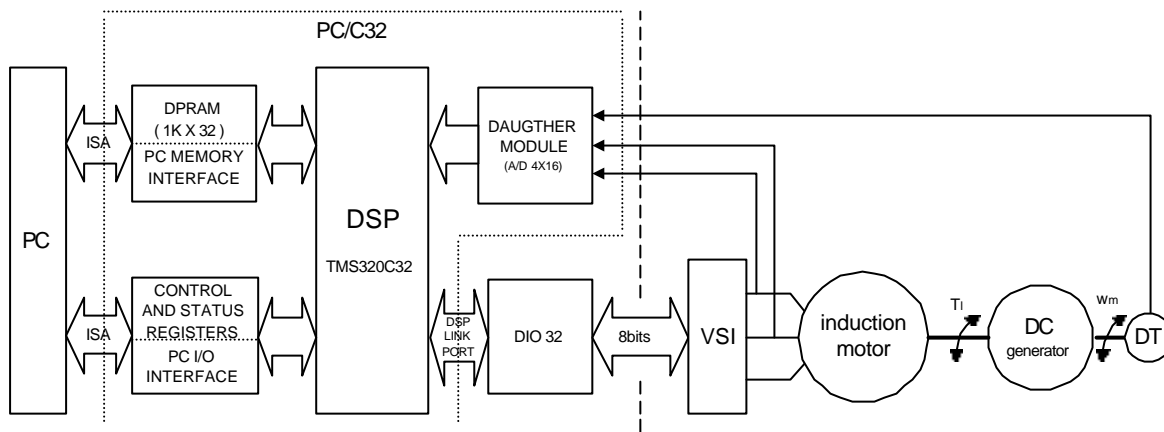


Figure 4.1. Experimental workbench. Its processors are PC and DSP. Communications between the drive and the PC/DSP are solved by means of 32 digital I/O lines and 4 ADC. DC generator is used as a load.

The experimental workbench is formed by the following described elements:

- Digital Signal Processor (DSP) TMS320C32. It is one of the processors that execute most of the programs of the control algorithm. It has got a self called "daughter module" that is composed by four analogue to digital converters of 16 bits, being its sampling frequency 50kHz. The processor has got as well an input/output board TTL of 32 bits. These two boards make possible and easier the communication between the induction motor drive and the DSP based processor system [LSI 1] [LSI 2] [LSI 3].
- Personal Computer (PC). This is the other processor that executes program code as well. It works as a host, not only due to the fact that it has inside all the DSP based boards, but also because it allows the edition and compilation of DSP and PC programs, keeping all the reference values and results in its memory.
- Voltage Source Inverter based on Isolated Gate Bipolar Transistors. This device supplies the induction motor generating a three phase voltage with variable both frequency and

Design of experimental induction motor drive system.

amplitude. Its main characteristics are its power that is 25kW and its maximum current 50A. It can be supplied in either 220 V or 380 V. There are the necessary protections such as current limit, over temperature, over DC link voltage, and IGBT saturation.

- Three-phase Induction motor_1kW. This machine was used for all the simulated results. Its main characteristics are as follows:

Star: 380V/2.8A

Delta: 220V/4.7A

Nominal mechanical power: $P_n = 1.35 \text{ CV} = 993.6 \text{ W}$

Nominal angular speed: $\omega_{mn} = 1420 \text{ r.p.m.} = 148.6 \text{ rd/s}$

Pair of poles: $P = 2$

Efficiency = 72%

$\cos(\phi) = 0.75$

$$\frac{T_{\text{START}}}{T_{\text{nom}}} = 2.2$$

$$\frac{T_{\text{MAX}}}{T_{\text{nom}}} = 2.4$$

Inertia moment: $J = 0.006 \text{ kg}\cdot\text{m}^2$

In this section is being presented the values per phase obtained performing both no load and locked rotor tests for the "T" induction steady state model.

Stator resistance: $R_1 = 7.13 \Omega$

Rotor resistance: $R_2 = 8.18 \Omega$

Magnetising inductance: $L_m = 0.6040 \text{ H}$

Leakage inductance: $L_1 = L_2 = 0.0301 \text{ H}$

Maximum and nominal values calculated using the identified parameters:

Nominal torque: $T_n = 6.7 \text{ N}\cdot\text{m}$

Shaft angular speed: $\omega_{mn} = 1378.4 \text{ r.p.m.} = 144.35 \text{ rd/s}$

Nominal slip: $s = 8.1 \cdot 10^{-2}$

RMS nominal magnetising current: $I_{mn} = 1.05 \text{ A}$

Start torque: $T_{\text{START}} = 12.46 \text{ N}\cdot\text{m}$

Maximum torque: $T_{MAX} = 16 \text{ N}\cdot\text{m}$ (at $\omega_{mMAX} = 851.94 \text{ r.p.m.}$)

Maximum slip speed: $s\omega_{sMAX} = 135.73 \text{ rad/s}$

RMS maximum stator current: $I_1 = 6.87 \text{ A}$

- Three-phase Induction motor_1.5kW. This machine not only has been used in all the simulation results but also in the experimental ones. Therefore, all the control strategies have been proved in this machine. This motor is mechanically jointed to the DC servomotor. Its main characteristics are as follows:

Star: 380V / 3.5A

Delta: 220V / 6A

Nominal mechanical power: $P_n = 1.5\text{kW}$

Nominal angular speed: $\omega_{mn} = 1450 \text{ r.p.m.} = 151.8 \text{ rd/s}$

Pair of poles: $P = 2$

Efficiency = 76.9%

$\cos(\phi) = 0.8$

In this section is being presented the values per phase obtained performing both no load and locked rotor tests for the "T" steady state induction motor model.

Stator resistance: $R_1 = 4.3 \Omega$

Rotor resistance: $R_2 = 5.05 \Omega$

Magnetising inductance: $L_m = 0.3056 \text{ H}$

Leakage inductance: $L_1 = L_2 = 0.0146 \text{ H}$

Maximum and nominal values calculated using the identified parameters:

Nominal torque: $T_n = 9.9 \text{ Nm}$

Shaft angular speed: $\omega_{mn} = 1400 \text{ r.p.m.} = 146.62 \text{ rd/s}$

Nominal slip: $s = 6.67 \cdot 10^{-2}$

- Permanent magnet DC servomotor. Its shaft is mechanically jointed to the Induction motor's one. Its function is to act as a mechanical load, changing the load torque to the Induction motor. Its main characteristics are as follows:

Manufacturer: Control Techniques.

Design of experimental induction motor drive system.

Type: Matador DCM 9B 30/20.

Armature voltage: 200V.

Maximum stable armature current: 20A.

Maximum peak armature current: 90A.

Armature resistance (at 25 °C): 0.31W.

Armature inductance: 2.3mH.

Number of poles: 4.

Type of isolation: F (100°C temperature increment).

Thermal time constant: 80minutes.

Maximum speed: 3000rpm.

Maximum stable torque: 11Nm.

Induced armature voltage: 57V/Krpm.

Torque constant at 25 °C: 0.55Nm/A(for $\omega_m = 0$ rd/s).

Rotor inertia: $10 \cdot 10^{-3}$ kgm².

Weight: 22kg

- Power Resistances. These resistances are electrically connected to the DC Generator absorbing different currents and consequently changing the load torque.
- Dynamometer. It gives a voltage proportional to the shaft speed. Its main characteristics are as follows:
 - Manufacturer: Radio-Energie.
 - Model: RE.0444 N1S 0.06 EG
 - Induced voltage: 0.06V/rpm
 - Maximum current: 0.18A.
 - Maximum angular speed: 10000rpm.
- Encoder. It is together with the DC motor. It supplies three signals and its complementary ones. Two of them are a square signals with one quarter of period delay. The third one gives one impulse each turn.
- Adaptive Signal Board. These circuits adapt the motor currents and the speed signals to the Analogue to Digital converters. There are some filters in order to reduce the noise keeping its delay as small as possible [LSI 3].

The system architecture based on two processors (see figure 4.1) allows the implementation of complex algorithms and the modular programming of the system being possible to change one processor program keeping the other. Both processors can perform the programs independently, exchanging the data by means of a DPRAM, which is a Dual Port Random Access Memory. One processor can interrupt the other. The PC can monitor the DSP by means of the interface based in the ISA bus. [LSI 1]

4.3 - Implementing DTC and FLDTC.

4.3.1 - Task distribution.

As it has been said previously, the system architecture allows the system to be reprogrammed easily. Therefore, many tasks were changed and proved without modifying the others.

Figure 4.2 shows the full schematic of the FLDTC. All blocks inside the dashed line are the ones corresponding to the fuzzy logic controllers. The PC performs some of these blocks. The rest of the tasks are performed by the DSP, which are mainly the DTC itself including the motor model and the consequent control of the real time.

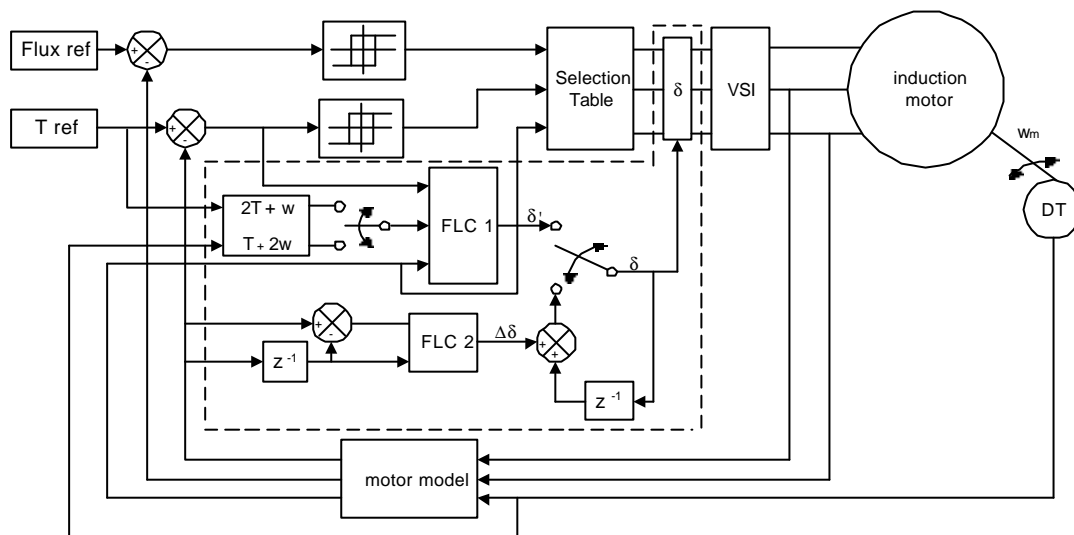


Figure 4.2. Schematic of the Fuzzy logic DTC. In dashed line is separated the novel fuzzy controller part, which is partially performed by the PC. The DSP performs the rest of the tasks controlling the real time.

It should be clear that despite the fact that there are two fuzzy logic controllers, just one fuzzy controller is used per iteration. Therefore, the computation capability of the real system won't be necessarily that much.

4.3.2 - Programming the system.

The DSP has been programmed using both C language and assembler. All the tasks, which its execution time was critical, have been programmed in assembler. Also, tasks that configure the DSP hardware and interfaces have been programmed in assembler.

The compiler allows mixed C and assembler code. [TII 2] [TII 3] [TII 4].

PC has been programmed in C language, due to the fact that its tasks are not critical regarding time [MAT 1]. The real time is performed by the DSP.

The DTC and the FLDTTC close the loop each $166\mu\text{s}$.

4.3.3 - Timing of the real implementation.

Once the real system is implemented, the first idea that must be taken into account is the delay due to the non ideal behaviour of the whole system. The most significant delays are introduced by the Analogue to Digital Converter (ADC) and the control algorithm. The ADC sampling frequency has been set to 20kHz, being the period $50\mu\text{s}$. In the `c_DTC`, as it can be seen in figure 4.3, the control algorithm is divided into three routines. These three routines are firstly attending the ADC interruption processing all the data, secondly the estimation of the torque and flux values and finally the DTC itself. All these routines take around $30\mu\text{s}$ to be executed. Therefore, there is a total delay of $80\mu\text{s}$ from the sampled data to the action of sending the new VSI state. Finally the data is saved in order to obtain the experimental results.

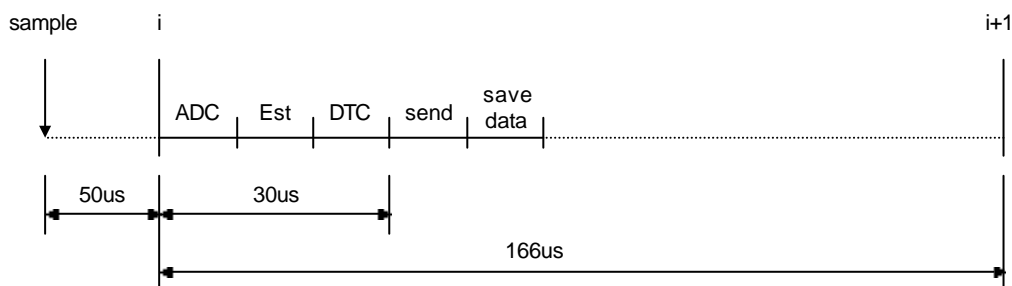


Figure 4.3. DTC timing. The DTC is executed each $166\mu\text{s}$. There is a delay of $80\mu\text{s}$ from the sampled data until the active state is sent.

In the FLDTTC the timing, shown in figure 4.4, is pretty similar to the classical DTC, already shown in figure 4.3. However, some differences are present, mainly due to the FLC. Then, once the active new state is sent, the FLC starts being executed. Because some parts of this controller are executed in the PC, the DSP waits until they are finished obtaining the duty cycle. Once the duty cycle is obtained, the timer is programmed. All this process takes $50\mu\text{s}$.

Design of experimental induction motor drive system.

Therefore, any duty cycle, which needs to change the active state before this time, is ignored. Therefore, not all the duty cycles are possible, being the minimum duty cycle 50% and the maximum 100%.

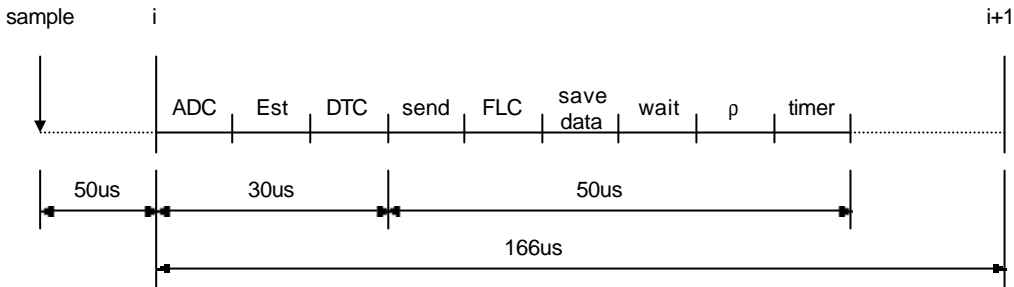


Figure 4.4 . FLDTTC timing. The FLDTTC is executed each 166μs. There is a delay of 80μs from the sampled data until the active state is sent. The Fuzzy Logic Controller needs 50μs to be calculated.

Seeing figures 4.3 and 4.4 the idea that both systems have the same delays in order to validate the comparison should be clear.

4.4 - Simulation of the real plant.

As it has been said in section 4.3.3, there are some limitations in the real plant. These limitations were not taken into account in the whole theoretical study realised in chapter 3. These limitations can be summarised as follows:

- The sample time can not be as small as wanted. In the real plant it is $166\mu\text{s}$.
- There is a delay of $30\mu\text{s}$ due to the software time execution.
- There is a delay of $50\mu\text{s}$ in the worst case due to the Analogue to digital conversion.
- The duty cycle values are limited due to the delay in the FLC execution. The real values are in the range of 50% up to 100%.

First three limitations are taken into account into the real simulation. It will be considered that its effect is similar to having a sample time of $166\mu\text{s}+30\mu\text{s}+50\mu\text{s}$, being equal to $246\mu\text{s}$. Therefore, the torque ripple is higher; in concrete is $246/100$ times higher; that is to say 2.46. All magnitudes related to the torque ripple should be pre scaled according to this factor. Therefore, 2.46 will divide all torque error FLC inputs and the torque hysteresis value will be 2.46 times bigger.

Simulations shown from figure 4.5 to 4.9 are done under these real conditions. All them should be compared with the experimental results obtained in chapter 5.

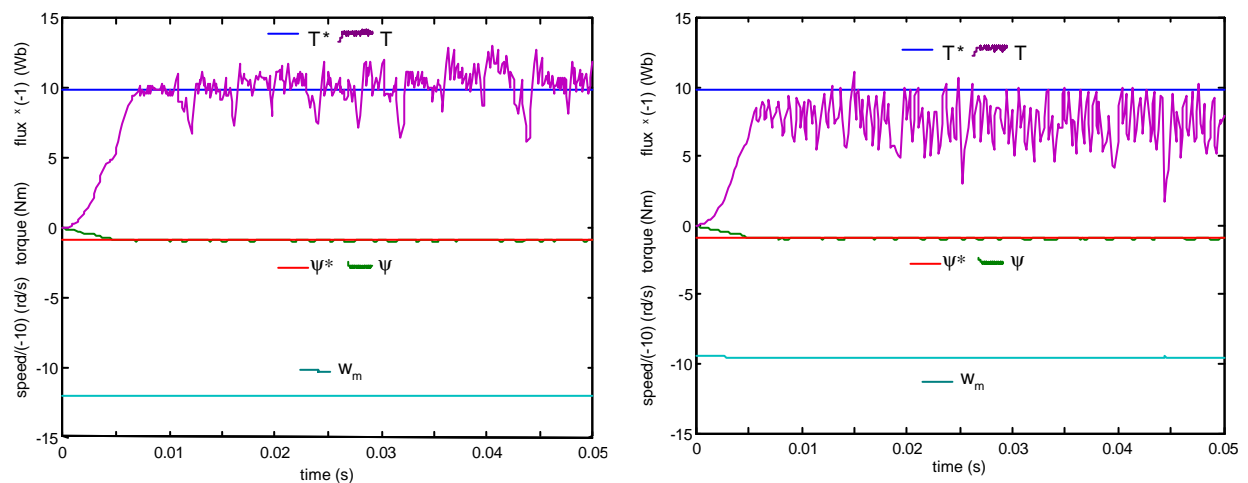


Figure 4.5. Stator flux, torque and speed motor_1.5kW responses in Fuzzy Logic DTC (left) and classical DTC (right). Torque reference value is 9.8Nm , i.e. $T=100\%T_n$. Torque load is being fixed by connecting a 4 ohms resistor to the DC generator. All real system limitations are taken into account.

Design of experimental induction motor drive system.

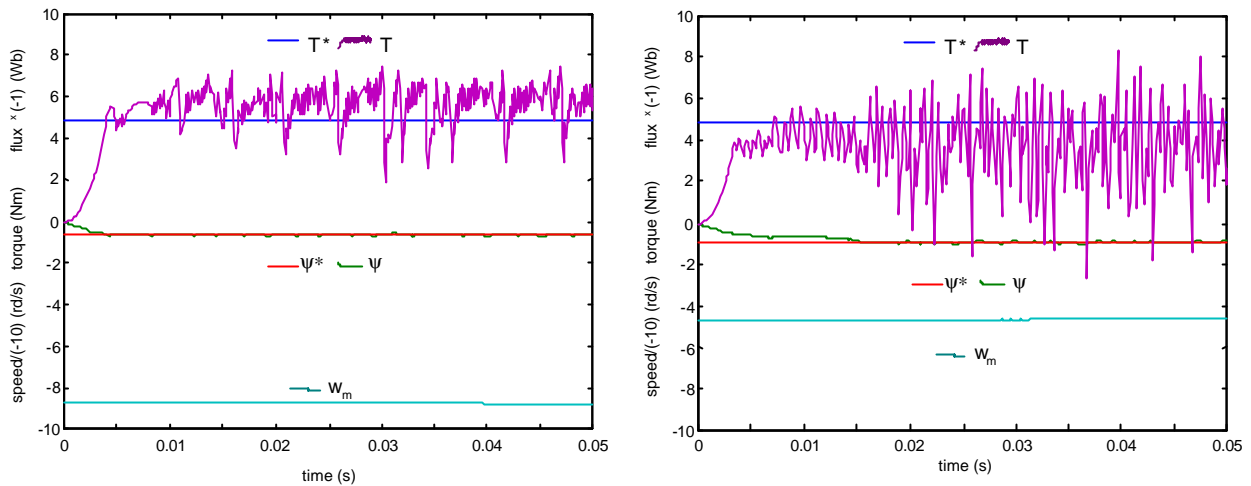


Figure 4.6. Stator flux, torque and speed motor_1.5kW responses in Fuzzy Logic DTC (left) and classical DTC (right). Torque reference value is 4.9Nm, i.e. $T=50\%T_n$. Torque load is being fixed by connecting a 4 ohms resistor to the DC generator. All real system limitations are taken into account.

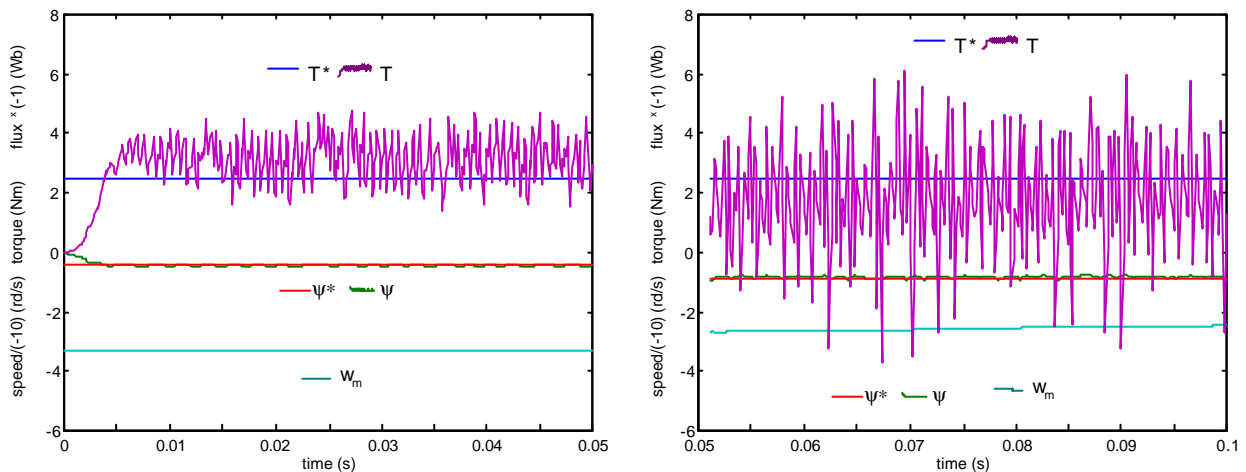


Figure 4.7. Stator flux, torque and speed motor_1.5kW responses in Fuzzy Logic DTC (left) and classical DTC (right). Torque reference value is 2.45Nm, i.e. $T=25\%T_n$. Torque load is being fixed by connecting a 4 ohms resistor to the DC generator. All real system limitations are taken into account.

From now on, all real simulations and all experimental results are just done or obtained from motor_1.5kW. From figures 4.5, 4.6 and 4.7 can be concluded that the FLDTTC is still working better than the classical DTC. Therefore, it is proved that the FLC can be adapted to any plant with its own characteristics and limitations, keeping its good performance. However, due to the limitations of the real system, both systems work worse when comparing these results with the one obtained in section 3.3.

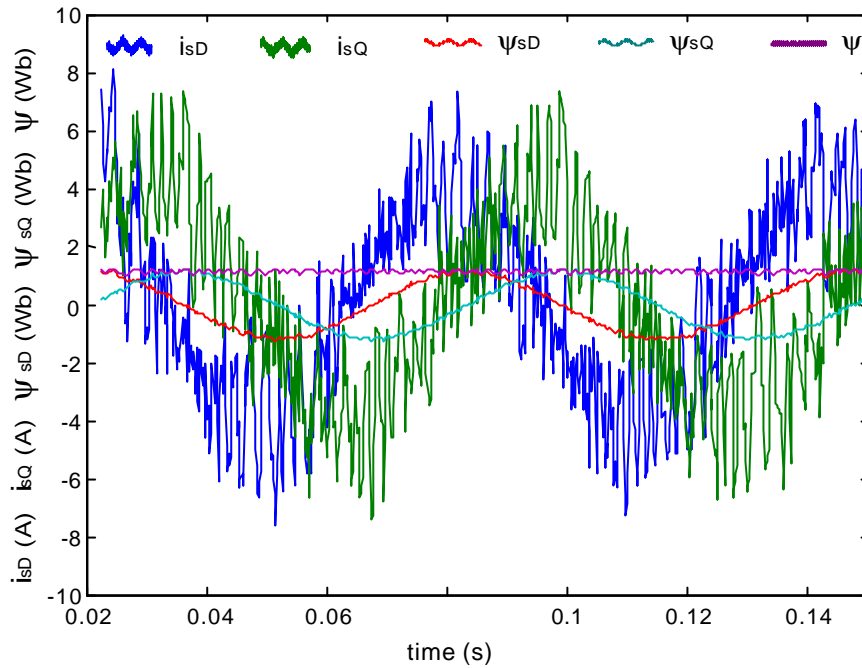


Figure 4.8 . D and Q current components. D and Q flux components and its module. All magnitudes correspond to the simulation realised in figure 4.6 right. That is to say, classical DTC, Torque reference value 4.9Nm, i.e. $T=50\%T_n$.

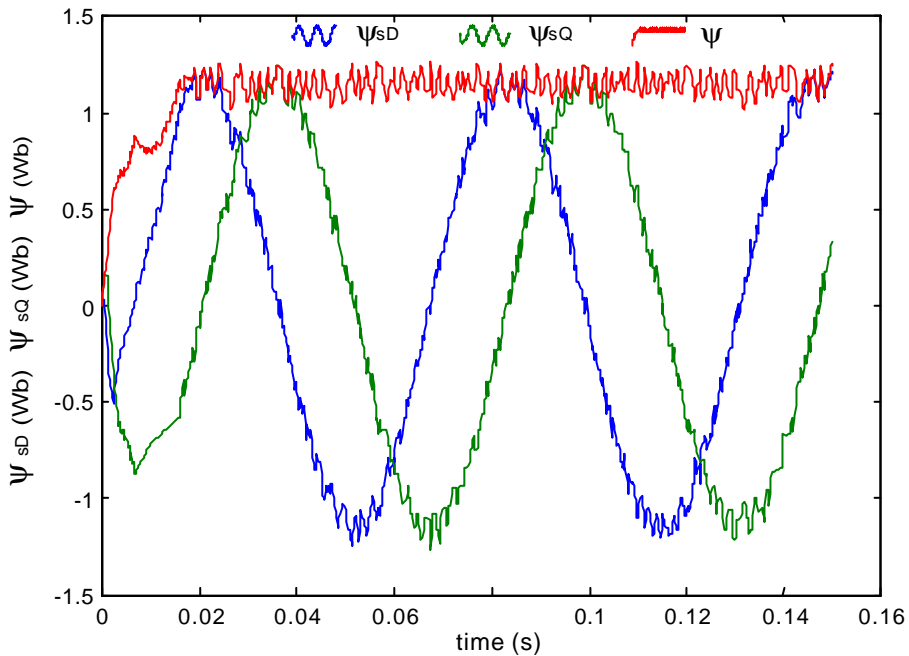


Figure 4.9. Figure 4.8 vertical zoom. D and Q stator flux components and its modulus value. Notice how once one component is zero, the other is equal to the modulus

4.5 - Interim conclusions.

This chapter has summarised the development of the equipment used for the experimental three phase induction motor drive.

It has been presented a parallel processing architecture with two processors (PC, DSP) running simultaneously. The DSP is based in the PC ISA bus, which gives a high immunity to conducted and radiated interference. This architecture solves the data exchange between processors and allows the experimentation of an AC motor control system with two processors that can execute two different programs in parallel. Reprogramming the system is considered to be one of the advantages of the system, because the changes in one processor program do not affect to the other. Also, the system is capable of acquiring external signals and of generating digital outputs signals [BED 2] [BED 3].

Finally, it has been pointed out the main problems due to the limitations of the real systems. It has been suggested a way to overcome the mentioned limitations keeping the proper performance of the system. Simulated results are shown to validate the work.